The Astrophysical Journal Letters, 714:L217–L221, 2010 May 10 doi:10.1088/2041-8205/714/2/L217

^{60}Fe AND ^{26}Al IN CHONDRULES FROM UNEQUILIBRATED CHONDRITES: IMPLICATIONS FOR EARLY SOLAR SYSTEM PROCESSES

R. K. Mishra[1], J. N. Goswami[1], S. Tachibana[2], G. R. Huss[3], and N. G. Rudraswami[1]
[1] Physical Research Laboratory, Ahmedabad-380009, India; goswami@prl.res.in
[2] Department of Earth and Planetary Sciences, University of Tokyo, 7-3-1 Hongo, Tokyo 113-0033, Japan
[3] Hawai'i Institute of Geophysics and Planetology, University of Hawai'i at Manoa, Honolulu, HI 96822, USA
Received 2009 June 13; accepted 2010 March 31; published 2010 April 14

ABSTRACT

The presence of about a dozen short-lived nuclides in the early solar system, including ^{60}Fe and ^{26}Al, has been established from isotopic studies of meteorite samples. An accurate estimation of solar system initial abundance of ^{60}Fe, a distinct product of stellar nucleosynthesis, is important to infer the stellar source of this nuclide. Previous studies in this regard suffered from the lack of exact knowledge of the time of formation of the analyzed meteorite samples. We present here results obtained from the first combined study of ^{60}Fe and ^{26}Al records in early solar system objects to remove this ambiguity. Chondrules from unequilibrated ordinary chondrites belonging to low petrologic grades were analyzed for their Fe–Ni and Al–Mg isotope systematics. The Al–Mg isotope data provide the time of formation of the analyzed chondrules relative to the first solar system solids, the Ca–Al-rich inclusions. The inferred initial ^{60}Fe/^{56}Fe values of four chondrules, combined with their time of formation based on Al–Mg isotope data, yielded a weighted mean value of $(6.3 \pm 2) \times 10^{-7}$ for solar system initial ^{60}Fe/^{56}Fe. This argues for a high-mass supernova as the source of ^{60}Fe along with ^{26}Al and several other short-lived nuclides present in the early solar system.

Key words: methods: analytical – nuclear reactions, nucleosynthesis, abundances

1. INTRODUCTION

Records of now-extinct short-lived radionuclides (SLRs) present at the time of formation of early solar system objects, such as Ca–Al-rich inclusions (CAIs), chondrules, and differentiated meteorites, provide high-resolution relative chronology of events leading to their formation (Russell et al. 2006; Halliday & Kleine 2006; Nyquist et al. 2009). The short-lived nuclide ^{60}Fe, which decays to ^{60}Ni with a half-life of 1.5 Myr, is a unique product of stellar nucleosynthesis (see, e.g., Meyer & Zinner 2006). A robust value of solar system initial (SSI) ^{60}Fe/^{56}Fe at the time of CAI formation would allow unambiguous identification of its stellar source and contribution from the same to the inventory of the other co-injected SLRs in the early solar system. A hint for the presence of ^{60}Fe in refractory CAIs, considered to be the first solid to form in the solar system, was reported more than two decades ago (Birck & Lugmair 1988). However, the lack of primary phases with high Fe/Ni ratio and possible presence of nucleogenic Ni isotope anomaly make CAIs unsuitable for inferring SSI ^{60}Fe. Differentiated meteorites, which provided direct evidence for the presence of live ^{60}Fe in early solar system (Shukolyukov & Lugmair 1993), are also prone to disturbance in Fe–Ni isotope systematics. Recent studies of Fe-rich phases (sulfides, oxides, and silicates) in matrix and chondrule from unequilibrated ordinary chondrites (UOCs) reported SSI ^{60}Fe/^{56}Fe values ranging from 2×10^{-7} to 1.6×10^{-6} (Tachibana & Huss 2003; Mostefaoui et al. 2005; Tachibana et al. 2006). However, the time of formation of the analyzed phases was not measured directly and plausible assumptions for the same were made to derive SSI ^{60}Fe/^{56}Fe. We report here results obtained from the first combined study of ^{26}Al and ^{60}Fe records in a set of UOC chondrules. The time of formation of the chondrules, relative to the CAIs, inferred from their Al–Mg isotope records, was used in conjunction with Fe–Ni isotope data to estimate SSI ^{60}Fe/^{56}Fe.

2. SAMPLES AND EXPERIMENTAL APPROACH

Chondrules from the UOCs, Semarkona, LEW86314, and Bishunpur were analyzed. Semarkona and Bishunpur are observed falls, while LEW86314 was collected in Antarctica. Studies of various indices of thermal metamorphism in bulk samples as well as individual chondrules (Huss et al. 2006, and references therein) suggest Semarkona (LL3.0) to be the least thermally affected sample followed by LEW86314 (L3.0) and Bishunpur (LL3.1). These UOCs have not experienced temperature exceeding 250–300°C during their residence in meteorite parent bodies (Huss et al. 2006) and chondrules in them should preserve pristine isotope records. Polished sections of these meteorites were studied using electron probe micro analyzer (EPMA) to identify chondrules (see Figure 1) hosting Fe-rich (olivine/pyroxene) and Al-rich (glassy mesostasis) phases. Al–Mg and Fe–Ni isotope studies of selected chondrules were carried out using a Cameca ims-4f ion microprobe at the Physical Research Laboratory (PRL), India, and a Cameca ims-1280 at the University of Hawaii (UH).

The experimental procedures adopted at PRL for Al–Mg isotope studies and results obtained for three chondrules were reported earlier (Rudraswami et al. 2008). The Fe–Ni isotope measurements were performed using the ims-4f at a mass resolution ($M/\Delta M$) of ~4000, sufficient to resolve major interferences at the masses of interest. Magnitude of unresolved hydride interference is at less than per mil level. A focused primary $^{16}O^{-}$ beam with intensity $\geqslant$5 nA was used to sputter secondary ions from the sample surface that are accelerated to 4.5 kV and energy sorted using an electrostatic analyzer. Ions within a small energy window (~25 eV) were mass analyzed using an electromagnet and ion counting was done using an electron multiplier. Each analysis consisted of 20 blocks of data, each of 5 cycles, through the mass sequence 56.7, ^{57}Fe, ^{60}Ni, and ^{62}Ni. Mass 56.7 was included to monitor dynamic background that ranged

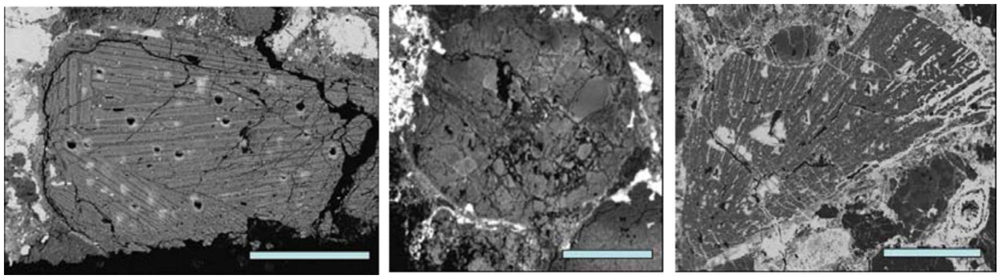

Figure 1. Backscattered electron images of representative UOC chondrules analyzed in this study: SEM39, a non-porphyritic bar chondrule (left), SEM21, a porphyritic chondrule (center), and LEW37, a non-porphyritic radial pyroxene chondrule (right). Ion beam produced sputter holes are visible in SEM39. Scale bar is 500 μm.

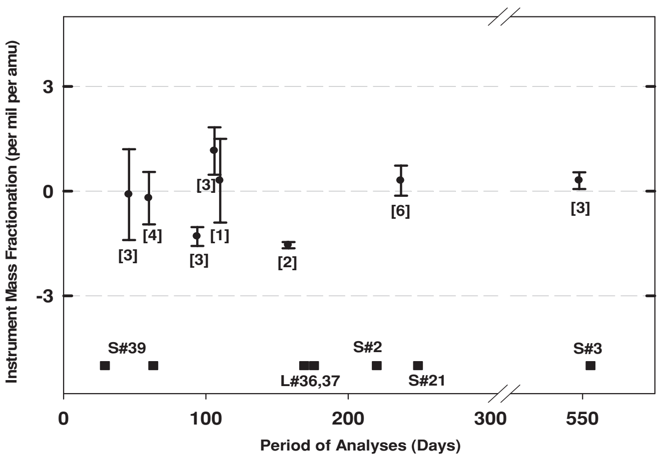

Figure 2. Instrumental mass fractionation, based on measured $^{62}Ni/^{60}Ni$ in terrestrial olivine, monitored at PRL during the period of this study. Number of analyses is shown within parenthesis. The bold squares indicate periods of acquiring Fe–Ni isotope data in chondrules (S: Semarkona; L: LEW86314).

Table 1
Inferred $(^{60}Fe/^{56}Fe)_0$ and $(^{26}Al/^{27}Al)_0$ in UOC Chondrules[a]

Sample	Initial ($^{60}Fe/^{56}Fe$)	Initial ($^{26}Al/^{27}Al$)	Source
Semarkona (LL3.0)			
SEM2	$<2.9 \times 10^{-7}$	$(5.5 \pm 0.34) \times 10^{-6}$	PRL[b]
SEM3	$(3.2 \pm 1.8) \times 10^{-7}$	$(6.9 \pm 5.8) \times 10^{-6}$	PRL
SEM21	$(4.9 \pm 2.6) \times 10^{-7}$	$(1.15 \pm 0.54) \times 10^{-5}$	PRL[b]
SEM39	$(4.3 \pm 2.4) \times 10^{-7}$	$<1.35 \times 10^{-5}$	PRL
SMK3–6	$(1.7 \pm 1.1) \times 10^{-7}$	$(7.2 \pm 2.8) \times 10^{-6}$	UH
SMK1–5	$(3.1 \pm 1.6) \times 10^{-7}$	$<6.7 \times 10^{-6}$	UH
SMK1–6	$<4.9 \times 10^{-7}$	$(6.6 \pm 2.0) \times 10^{-6}$	UH
Bishunpur (LL3.1)			
BIS-32	$(1.9 \pm 1.1) \times 10^{-7}$	$<3.5 \times 10^{-6}$	UH
LEW86314 (L3.0)			
LEW36	$(4.2 \pm 2.8) \times 10^{-7}$	$(1.63 \pm 0.72) \times 10^{-5}$	PRL[b]
LEW37	$(4.9 \pm 3.8) \times 10^{-7}$	—[c]	PRL

Notes.
[a] Errors are 2σ.
[b] Al–Mg data from Rudraswami et al. (2008).
[c] No suitable phase found for Al–Mg isotope analysis.

from 0.01 to 0.02 cps. Typical count times were 10 s (56.7), 1 s (^{57}Fe), 10 s (^{60}Ni), and 50 s (^{62}Ni) and an analysis lasted about 2 hr. Data for multiple analyses, conducted on the same spot or multiple spots in the same phase (olivine or pyroxene), were combined as long as the count rates and Fe/Ni ratio remained steady to improve precision of the measured isotope ratios. Instrument mass fractionation was monitored by analyzing terrestrial olivine standards (San Carlos and Vernadsky olivine) during and in between sample runs over the entire period of study; the values are close to one per mil per amu (Figure 2). This is also corroborated by the data for low Fe/Ni phases in the analyzed chondrules. The relative ion yield of Fe and Ni from olivine and pyroxene has been extensively studied earlier (Kita et al. 1998; Sugiura et al. 2006) and indicated a dependence on Fe content and the nature of primary ion beam ($^{16}O^-$and $O_2{}^-$). Based on our data for the Vernadsky olivine standard with Fe content (16%) close to those for the analyzed chondrule phases (11%–18%), we adopt a value of unity for relative Ni/Fe ion yield.

At UH, Fe–Ni isotope measurements were made using a Cameca ims-1280. A focused, 15–30 μm, 3–5 nA, primary O^- beam was rastered over a 20 × 20 μm square on samples and standards. The instrument was operated at 10 kV with a 50 eV energy window and a mass resolving power of ∼5000, sufficient to resolve all interferences except for hydrides. Secondary ions ($^{57}Fe^+$, $^{60}Ni^+$, $^{61}Ni^+$, and $^{62}Ni^+$) were counted on a monocollector electron multiplier for 0.3, 3, 15, and 5 s in each cycle. Each spot was measured for 2 hr. Data are corrected for electron multiplier background (0.02 cps) and deadtime (29.5 ns). Instrumental mass fractionation was corrected internally using the measured $^{62}Ni/^{61}Ni$ ratio. Contributions of interferences of hydrides to count rates of nickel isotopes were less than 1‰ (see Tachibana et al. 2006, 2007 for additional details). The Mg isotope analyses of the Al-rich chondrule glass were conducted using a 0.1 nA focused O^- beam. Secondary ions ($^{24}Mg^+$, $^{25}Mg^+$, and $^{26}Mg^+$) were collected on the monocollector electron multiplier and $^{27}Al^+$ was measured on the monocollector Faraday cup. Miyake-jima plagioclase and San Carlos olivine were used as standards.

3. RESULTS AND DISCUSSION

Presence of both high Al/Mg and high Fe/Ni phases in individual chondrule is rare. In general, porphyritic chondrules hosting glassy phase (mesostasis) with high Al/Mg are devoid of high Fe/Ni phase, while reverse is the case for non-porphyritic chondrules. Based on EPMA data for more than a few hundred chondrules, we selected about two dozen chondrules from the three UOCs for this study. In 10 of them we could obtain data for either Al–Mg or Fe–Ni isotope system or both (see Table 1). Four chondrules (SEM3, SEM21, SMK3–6, and LEW36) yielded data for both; the Fe–Ni isotope data for these are shown in Figure 3. The initial $^{60}Fe/^{56}Fe$ at the time of formation of these chondrules, defined by the slope of the best-fit line through each data set, along with their inferred initial $^{26}Al/^{27}Al$ (this study and Rudraswami et al. 2008) are also shown in the figure. In three additional chondrules, we could obtain initial $^{60}Fe/^{56}Fe$; however, they yielded only upper limits for initial $^{26}Al/^{27}Al$.

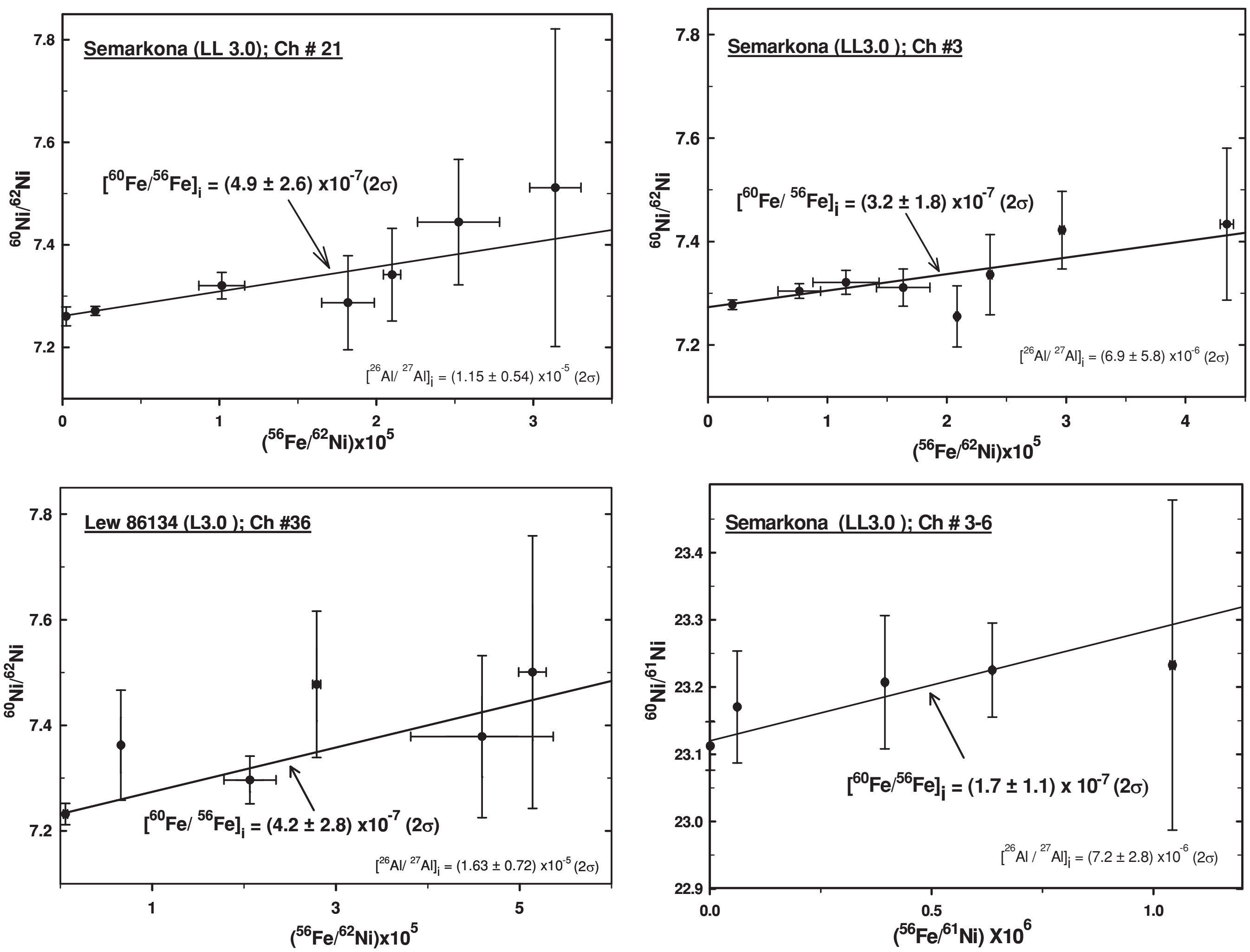

Figure 3. Fe–Ni three isotope plots for chondrules (SEM21, LEW36, SEM3, and SMK3–6). The inferred initial (^{60}Fe/^{56}Fe) and (^{26}Al/^{27}Al) values at the time of formation of these chondrules are also shown. Error bars are 2σ. Initial (^{26}Al/^{27}Al) for SEM21 and LEW36 are from Rudraswami et al. (2008).

Chondrules are products of melting of precursor microscopic solids followed by rapid cooling in the solar nebula (Scott & Krot 2005). The melting events homogenized the isotopic compositions of the chondrules, resetting the isotopic clocks, and the inferred initial ^{26}Al/^{27}Al and ^{60}Fe/^{56}Fe represent values at the time of their formation. The observed spread in initial ^{26}Al/^{27}Al values (0.55–1.6) $\times 10^{-5}$, combined with the canonical ^{26}Al/^{27}Al value of 5×10^{-5} for CAIs, suggest that these chondrules formed between 1.2 and 2.1 Ma after CAIs. If we consider the initial ^{60}Fe/^{56}Fe values for the four chondrules (Figure 3) and their mean time of formation, they yield SSI ^{60}Fe/^{56}Fe values ($\pm 2\sigma$) of $(8.3 \pm 4.7) \times 10^{-7}$ (SEM3), $(4.3 \pm 2.8) \times 10^{-7}$ (SMK3–6), $(7.2 \pm 4.8) \times 10^{-7}$ (LEW36), and $(9.9 \pm 5.3) \times 10^{-7}$ (SEM21) and define a weighted average SSI ^{60}Fe/^{56}Fe value of $(6.3 \pm 2) \times 10^{-7}$. This value is within the range inferred in an earlier study, *assuming* a time interval of 1.5–2 Ma between the formation of CAIs and the analyzed UOC chondrules (Tachibana et al. 2006). Our results do not support the SSI value of $\sim 1.6 \times 10^{-6}$ inferred from the analysis of an Allende CAI (Birck & Lugmair 1988). It is also at variance with values inferred from studies of UOC sulfides of unknown formation time (Tachibana & Huss 2003; Mostefaoui et al. 2005). We note that during the course of this study a revised half-life of 2.6 Ma for ^{60}Fe has been proposed (Rugel et al. 2009). If true, this will lower the SSI ^{60}Fe/^{56}Fe value obtained in this study by $\sim$30% and does not alter the above inferences.

The use of various SLRs as relative chronometers of early solar system events is based on the assumptions that they were homogeneously distributed in the early solar system and characterized by unique SSI abundances. The above estimate of SSI ^{60}Fe/^{56}Fe, using ^{26}Al as a time marker, thus requires that the SLRs ^{60}Fe and ^{26}Al satisfy these assumptions. Self-consistent chronology obtained for solar system events based on Pb–Pb, ^{182}Hf–^{182}W, ^{53}Mn–^{53}Cr, and ^{26}Al–^{26}Mg isotope systems (Russell et al. 2006; Halliday & Kleine 2006; Nyquist et al. 2009) suggest that the SLRs, ^{26}Al, ^{53}Mn, and ^{182}Hf, were homogeneously distributed in the early solar system and have well-defined SSI abundances. However, based on the observed apparent deficits in ^{60}Ni from meteorites that formed very early in solar system history, Bizzarro et al. (2007) suggested a late injection of ^{60}Fe into the solar system, relative to ^{26}Al, from a massive star. It was proposed that ^{26}Al was injected via stellar wind during the early evolution of the star, and ^{60}Fe, about a million year later, when it ended its life as a Type Ib/Ic supernova. If true, the SLR ^{182}Hf, which is co-produced with ^{60}Fe in stellar nucleosynthesis (Meyer 2005; Meyer & Zinner 2006), would also be injected late into the solar system. A very systematic study of Fe–Ni isotope records of various meteorites (Dauphas et al. 2008) could not reproduce the results of Bizzarro

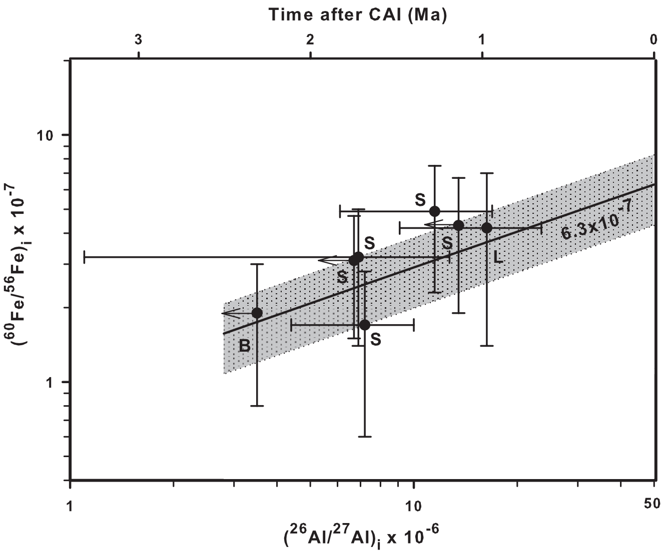

Figure 4. Initial ($^{60}Fe/^{56}Fe$) vs. initial ($^{26}Al/^{27}Al$) at the time of formation of the analyzed UOC chondrules (error bars are 2σ). In three of the chondrules, initial ($^{26}Al/^{27}Al$) are upper limit estimates. The scale on top provides the time of formation of the chondrules, relative to CAIs. The solid line indicates the expected trend for the SSI ($^{60}Fe/^{56}Fe$) value obtained in this study, assuming co-injection of ^{26}Al and ^{60}Fe; the shaded region represents the error envelope (S: Semarkona; L: LEW86314; B: Bishunpur).

et al. (2007) and negates the late injection hypothesis for ^{60}Fe. Further, records of ^{182}Hf and ^{26}Al in CAIs and later formed angrites of known formation ages are also consistent with their homogeneous distribution in the early solar system (Burkhardt et al. 2008; Nyquist et al. 2009). These results argue for co-injection and homogeneous distribution of ^{60}Fe, ^{26}Al, and ^{182}Hf in the early solar system and validate our approach for inferring SSI $^{60}Fe/^{56}Fe$ based on combined Fe–Ni and Al–Mg isotope data for chondrules.

A plot of initial $^{60}Fe/^{56}Fe$ versus initial $^{26}Al/^{27}Al$ for the analyzed chondrules is shown in Figure 4. The time of formation of the chondrules, relative to CAIs, is also indicated. If ^{26}Al and ^{60}Fe were co-injected into the nascent solar system and distributed homogeneously within the solar system, the data should fall along a linear trend in this log–log plot. In spite of the relatively large error and upper limit values for $^{26}Al/^{27}Al$ in several cases, the data display such a trend and support co-injection of these two SLRs. This makes ^{60}Fe a potential heat source, along with ^{26}Al, for early thermal metamorphism of planetesimals (see, e.g., Yoshino et al. 2003). Our results suggest that with improved analytical precision in measurements of Fe–Ni isotope systematics, ^{60}Fe could be a viable chronometer for early solar system events.

^{60}Fe is a product of *s*-process nucleosynthesis via neutron capture and both a core-collapse supernova (SN-II) and a high-mass ($\geqslant 5\ M_\odot$) thermally pulsing (TP)-asymptotic giant branch (AGB) star could be a source of this nuclide. Low-mass AGB stars do not attain the temperature required for activation of the high-density ^{22}Ne neutron source needed for effective production of ^{60}Fe (Wasserburg et al. 1995, 2006). Contemporaneous injection of ^{41}Ca and ^{26}Al from a stellar source into the protosolar cloud had been proposed earlier (Sahijpal et al. 1998, 2000) and the present study suggests co-injection of ^{26}Al and ^{60}Fe. Thus, any proposed stellar source should be able to account for the inferred SSI $^{60}Fe/^{56}Fe$ as well as those for $^{26}Al/^{27}Al$ and $^{41}Ca/^{40}Ca$ reported previously (see, e.g., Goswami et al. 2005). The same source should ideally account for the SSI abundances of other SLRs (e.g., ^{182}Hf and ^{53}Mn) that are also homogeneously distributed in the early solar system along with ^{26}Al and ^{60}Fe (Dauphas et al. 2008; Nyquist et al. 2009). Identification of a plausible stellar source is based on its ability to concurrently match the SSI abundance of multiple SLRs by considering injection of a specific amount of freshly synthesized stellar material, containing the SLRs, into the protosolar cloud and assuming a time interval between their synthesis and eventual incorporation into the first solar system solids. Studies of nucleosynthesis yields from a massive ($\geqslant 25\ M_\odot$) star that ends its life as a Type-II supernova suggest that it could be a plausible source for multiple SLRs. However, it is necessary to invoke mixing and fall back of material in the inner region of such stars as well as an injection mass cut for ejected stellar material containing freshly synthesized SLRs (Meyer 2005; Meyer & Adams 2006; Takigawa et al. 2008). The possibility of a high-mass TP-AGB star as a source of SLRs present in the early solar system has also been considered by Wasserburg et al. (2006) and Trigo-Rodrigues et al. (2009). Reasonable match with SSI abundances (within a factor of 2) could be obtained for ^{26}Al, ^{41}Ca, and ^{60}Fe. However, both the amount of injected stellar material and the time interval between the production of these SLRs and their incorporation into solar system solids differ significantly in these two approaches. Further, unlike the case of massive stars, whose association with star-forming regions is well documented, the probability of association of a high-mass AGB star with star-forming regions is extremely small, $\leqslant 10^{-5}$ (see, e.g., Huss et al. 2009), making such an association very unlikely. It is also necessary to invoke additional contribution from a massive star to explain the presence of the SLRs ^{182}Hf and ^{53}Mn that are not products of nucleosynthesis in AGB stars. Injection of freshly synthesized material from an SN associated with a massive star remains the most plausible source for ^{60}Fe and several other SLRs present in the early solar system.

REFERENCES

Birck, J. L., & Lugmair, G. W. 1988, Earth Planet. Sci. Lett., 90, 131

Bizzarro, M., Ulfbeck, D., Trinquier, A., Thrane, K., Connelly, J. N., & Meyer, B. S. 2007, Science, 316, 1178

Burkhardt, C., Kleine, T., Bourdon, B., Palme, H., Zipfel, J., Friedrich, J. M., & Ebel, D. 2008, Geochim. Cosmochim. Acta, 72, 6177

Dauphas, N., et al. 2008, ApJ, 686, 560

Goswami, J. N., Marhas, K. K., Chaussidon, M., Gounelle, M., & Meyer, B. S. 2005, in ASP Conf. Ser. 341, Chondrites and the Protoplanetary Disk, ed. A. N. Krot, E. R. D. Scott, & B. Reipurth (San Francisco, CA: ASP), 485

Halliday, A. N., & Kleine, T. 2006, in Meteorites and the Early Solar System II, ed. D. S. Lauretta & H. Y. McSween Jr. (Tucson, AZ: Univ. Arizona Press), 775

Huss, G. R., Meyer, B. S., Srinivasan, G., Goswami, J. N., & Sahijpal, S. 2009, Geochim. Cosmochim. Acta, 73, 4922

Huss, G. R., Rubin, A. E., & Grossman, J. N. 2006, in Meteorites and the Early Solar System II, ed. D. S. Lauretta & H. Y. McSween Jr. (Tucson, AZ: Univ. Arizona Press), 567

Kita, N. T., Togashi, S., Morishita, Y., Terashima, S., & Yurimoto, H. 1998, Antarct. Meteor. Res., 11, 103

Meyer, B. S. 2005, in ASP Conf. Ser. 341, Chondrites and the Protoplanetary Disk, ed. A. N. Krot, E. R. D. Scott, & B. Reipurth (San Francisco, CA: ASP), 515

Meyer, B. S., & Adams, D. C. 2006, Lunar Planet. Sci., 37, 1403

Meyer, B. S., & Zinner, E. 2006, in Meteorites and the Early Solar System II, ed. D. S. Lauretta & H. Y. McSween Jr. (Tucson, AZ: Univ. Arizona Press), 69

Mostefaoui, S., Lugmair, G. W., & Hoppe, P. 2005, ApJ, 625, 271

Nyquist, L. E., Kleine, T., Shih, C.-Y., & Reese, Y. D. 2009, Geochim. Cosmochim. Acta, 73, 5115

Rudraswami, N. G., Goswami, J. N., Chattopadhyay, B., Sengupta, S. K., & Thapliyal, A. P. 2008, Earth Planet. Sci. Lett., 274, 93

Rugel, G., et al. 2009, Phys. Rev. Lett., 103, 072502

Russell, S. S., Hartmann, L., Cuzzi, J. N., Krot, A. N., Gounelle, M., & Weidenschilling, S. J. 2006, in Meteorites and the Early Solar System II, ed. D. S. Lauretta & H. Y. McSween Jr. (Tucson, AZ: Univ. Arizona Press), 233
Sahijpal, S., Goswami, J. N., & Davis, A. M. 2000, Geochim. Cosmochim. Acta, 64, 1989
Sahijpal, S., Goswami, J. N., Davis, A. M., Grossman, L., & Lewis, R. S. 1998, Nature, 391, 559
Scott, E. R. D., & Krot, A. N. 2005, in ASP Conf. Ser. 341, Chondrites and the Protoplanetary Disk, ed. A. N. Krot, E. R. D. Scott, & B. Reipurth (San Francisco, CA: ASP), 15
Shukolyukov, A., & Lugmair, G. W. 1993, Science, 259, 1138
Sugiura, N., Miyazaki, A., & Yin, Q.-Z. 2006, Earth Planets Space, 58, 1079
Tachibana, S., & Huss, G. R. 2003, ApJ, 588, L41
Tachibana, S., Huss, G. R., Kita, N. T., Shimoda, G., & Morishita, Y. 2006, ApJ, 639, L87
Tachibana, S., Huss, G. R., & Nagashima, K. 2007, Lunar Planet. Sci. Conf., 38, 1709
Takigawa, A., Miki, J., Tachibana, S., Huss, G. R., Tominaga, N., Umeda, H., & Nomoto, K. 2008, ApJ, 688, 1382
Trigo-Rodrigues, J. M., Garcia-Hernandez, D. A., Lugaro, M., Krakas, A. I., Raai, M., Lario, P. G., & Manchado, A. 2009, Meteorit. Planet. Sci., 44, 627
Wasserburg, G. J., Busso, M., Gallino, R., & Nollett, K. M. 2006, Nucl. Phys. A, 777, 5
Wasserburg, G. J., Gallino, R., Busso, M., Goswami, J. N., & Raiteri, C. M. 1995, ApJ, 440, L101
Yoshino, T., Michael, J. W., & Tomoo, K. 2003, Nature, 422, 154